

Ibrahim Olatunji RAUFU^{1A*}, Herbert TATA^{1B}, Solihu OLAOSEGBA²

¹Department of Surveying and Geoinformatics, Federal University of Technology, Akure, Nigeria, raufuibrahimolatumji@gmail.com, htata@futa.edu.ng, ^{1A}<https://orcid.org/0000-0003-3474-8618>,

^{1B}<https://orcid.org/0000-0002-9755-1612>

²Department of Surveying and Geoinformatics, Federal School of Surveying Oyo, Nigeria, olaosegba@fss-oyo.edu.ng, ²<https://orcid.org/0000-0002-6212-1081>

<https://doi.org/10.23939/istcgcap2023.98.063>

MODELLING LOCAL GEOID UNDULATIONS USING UNMANNED AERIAL VEHICLES (UAVS): A CASE STUDY OF THE FEDERAL UNIVERSITY OF TECHNOLOGY, AKURE, NIGERIA

The study was aimed at developing a geoid model using Unmanned Aerial Vehicle (UAV) technology. To accomplish this, a UAV was deployed to capture imagery of the study area from a height of 150m, with a ground resolution of 4.19cm. A total of 3737 images were obtained, covering an area of 725.804 hectares. The existing ellipsoidal and orthometric heights were used to georeference the acquired images. For the analysis, 35 points were utilized, with 20 points designated as ground control points (GCPs) and the remaining 15 points as check points (CPs). Using the UAV-derived Digital Terrain Models (DTMs), a dataset comprising 18,492 points was generated for both ellipsoidal (h) and orthometric (H) heights. The differences between these heights, referred to as geoid heights (N), were calculated as $N = h - H$ for all 18,492 points. These geoid heights were subsequently employed to generate a geoid model, including contour maps and 3D maps, of the study area. To assess the accuracy of the UAV-derived geoid heights, a root mean square error (RMSE) analysis was performed by comparing them with the existing geoid heights and was found to be 0.113 m. The scientific novelty and practical significance are in the development of a local geoid model of the study area with centimetre-level precision. Thus, the output of this study can be used for a wide range of applications, including land management, construction, and environmental impact assessments in the study area.

Key words: geoid, UAV, DTM, ellipsoidal height, orthometric height

Introduction

In the early stages of human intellectual development, the question of "what is the earth, its size, and shape" emerged as one of the first issues that needed to be resolved. Geodesy deals with the measurement and monitoring of Earth's dimensions, shape, gravity field, and the precise determination of point locations on its surface (NOAA, 2021). Thus, the basic geodetic surfaces that describe the earth consist of its actual surface, the ellipsoid that provides the best mathematical approximation of the Earth's shape, and the geoid, which represents an equipotential surface perpendicular to the direction of gravity at all points [Oluyori et al., 2018]. The physical surface of the earth contains a variety of landforms like plains, valleys, mountains, water features, etc. [Prasad, 2015] but its main problem as a reference surface for position, dimension, and shape determination is its irregularity [Agajelu, 2018]. The geoid on the other hand is an equipotential level surface of the earth's gravity field closely approximated by the mean sea level under ideal conditions of ocean waters, and the extension of that surface underneath the continents to make it continuous and covers the whole earth [Agajelu,

2018]. The geoid plays a crucial role in engineering by being widely applied to define physical heights [Sanso et al., 2019] and it serves as a reference surface or datum that refines the fundamental equations of motion for the Earth's fluid envelopes [Albayrak et al., 2020]. Acknowledging the value of the geoid as a true representation of the shape of the earth makes modelling such a shape even more crucial for a variety of applications.

Geoid modelling development incorporates geodetic, gravimetric, and astrogeodetic techniques [Albayrak et al., 2020]. For the precise definition of a geoid, the Global Navigation Satellite System/levelling (GNSS/levelling) method, a geodetic technique, can be utilized. This approach involves converting GNSS-derived ellipsoidal heights (h) into orthometric heights (H). Instead of levelling, well-established geoid models can be employed to calculate orthometric heights. These geoid models enable the computation of geoid height (N), which represents the difference between ellipsoidal and orthometric height values ($N = h - H$). Subsequently, orthometric heights can be computed by using the geoid heights and known ellipsoidal heights [Jekeli et al., 2012].

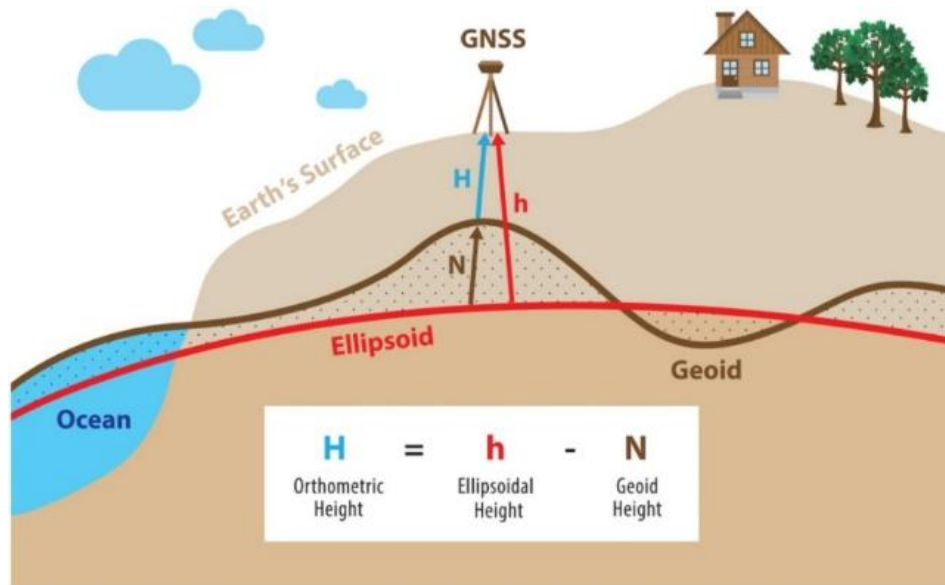


Fig. 1. Relationship between earth surface, geoid and ellipsoid (Albayrak et al., 2020).

Several methodologies have been adopted in modelling geoid globally, regionally, and locally. The methodologies range from terrestrial to airborne and to space-borne. Al-kragy et al. (2014) employed the GPS/levelling technique to model local geoid and to evaluate the performance of several Global Geopotential Models (GGMs) in Egypt. The result shows that the best model for local geoid in the study area was that of the 2nd-order polynomial and a standard deviation of $\pm 0.050\text{m}$ was obtained which exceeds the precision of all tested GGMs models over the study area. Erol end Erol (2020) examined four distinct surface interpolation techniques aimed at local geoid modelling in the western region of Turkey. The methodologies evaluated encompass multivariable polynomial regression (MPR), least-squares collocation (LSC), bivariate (BIVAR) interpolation, and wavelet neural networks (WNN). The result obtained shows that the BIVAR technique demonstrated a better performance with an accuracy of 2.65 cm, surpassing even a gravimetric geoid model in the study area. In another study by Maglione et al. (2018), the accuracy of global geoid height models in a local area was studied in the Campania region of Italy. The result shows that the global geoid height models are often not suitable for local applications with RMS values of 1.157m, 0.444m, and 0.288m obtained for EGM84, EGM96, and EGM2008 respectively. Erol et al. (2020) assess the performance of photogrammetry methods for determining local geoid model in Turkey. The study

employs direct georeferenced airborne LiDAR and indirect georeferenced UAV photogrammetry-derived point clouds to generate DTMs in ellipsoidal and geoidal vertical datums. The local geoid model was estimated as the variation between the constructed DTMs with an accuracy of 9.2 cm. In a prior study conducted by Raufu & Tata (2021), the accuracy of three polynomial geoid models was evaluated in Akure, Nigeria. The best-fitting geoid model yielded a standard deviation of 14.7 cm. In their study, Belay et al. (2021) employed the remove-compute-restore (RCR) procedure and the least-squares collocation (LSC) method to formulate a gravimetric geoid model for Ethiopia. The accuracy of this model was evaluated using geometric geoid heights, resulting in a precision of 13 cm. However, due to the required level of accuracy, global and regional geoid models may not be suitable for local applications such as engineering and construction. The use of ellipsoidal heights derived from GNSS requires the use of a geoid model to transform them into orthometric heights. However, Odera & Fakuda (2015) opined that global models tend to be overly generalized for localized applications. Furthermore, the absence of a national geoid model in Nigeria, as emphasized by [Raufu & Tata, 2021; Oluyori et al., 2018], highlights the significance of developing local geoid models for precise localized applications.

Over the past few years, the study area has witnessed tremendous structural development. To en-

sure adequate and sustainable development, the establishment of a reliable reference model for height determination has become an essential priority. However, the traditional methods of extending orthometric height such as terrestrial survey methods, can be time-consuming, expensive, and tedious. The use of gravimeters is also costly, and it is only feasible to occupy a limited number of points for interpolation purposes. In light of these challenges, it was essential to adopt an alternative approach that could effectively model the entire study area in a relatively short period. This necessity led to the adoption of Unmanned Aerial Vehicles (UAVs) for the purpose of modelling geoidal undulation for the study area.

The utilization of UAVs presents a promising solution for the acquisition of multi-temporal aerial stereo photos and high-resolution digital surface models [Chi et al., 2016]. Therefore, by leveraging UAVs and having a sufficient number of Ground Control Points (GCPs), it is anticipated that accurate local geoid modelling can be achieved. Therefore, this research aims to make the most of these advancements and develop a local geoid model for the study area.

Unmanned Aerial Vehicle technology in locational data acquisition

The application of UAVs for remote data collection has witnessed significant advancements in recent years [Quaye-Ballard et al., 2020] and it has become a new surveying technique for acquiring spatial information [Yeh et al., 2018]. This practice of employing UAVs in surveying has gained global popularity in recent times [Christiansen et al., 2017; Gonzalez et al., 2016; Turner et al., 2016]. While specialized UAVs equipped with high-accuracy Global Positioning System (GPS) for mapping purposes are available, they come at a higher cost. However, consumer-grade UAVs, which are more affordable, user-friendly, and readily accessible, are being employed for various applications such as topographical mapping and generation of precise digital elevation model (DEM) [Polat & Uysal, 2017]. By leveraging GPS and GCPs, these consumer-grade UAVs have facilitated topographical surveying and have reduced both time and cost in acquiring data for inaccessible land areas, particularly through integration with

GPS and Geographic Information System (GIS) techniques [Quaye-Ballard et al., 2020]. The accuracy of the topographic map can be achieved as low as 5cm [Quaye-Ballard et al., 2020].

Considering the cost-effectiveness and sufficient accuracy of UAV technology in height determination, and recognizing that geoid modelling relies on precise height data (especially when using terrestrial methods), we decided to use UAV technology for geoidal undulation modelling in this study.

Aim of the study

The aim of this study is to develop a local geoid undulation model of the Federal University of Technology, Akure, using a UAV technology. The research was conducted for the purpose of using the model for important projects that require precise height information, such as urban planning, infrastructure design, and flood modelling in the institution.

Study area

The study area chosen for this research is the Federal University of Technology Akure (FUTA), located in Akure South Local Government Area of Ondo State, in the southwestern region of Nigeria. Geographically, it is situated between latitudes $07^{\circ} 18'$ to $07^{\circ} 20'$ and longitudes $05^{\circ} 06'$ to $05^{\circ} 09'$. The study area covered a total area of 577.97 hectares as shown in Fig. 2 and the distribution of ground control points is shown in Fig. 3.

Method

The methodology employed in this study includes three main components: GPS observation using South Differential GNSS receivers, precise leveling observation using a Leica DNA03 digital level instrument, and UAV mapping using a DJI Phantom 4 Pro UAV. A total of thirty-five (35) control points were observed for the GNSS and leveling operations, with twenty-nine (29) pre-existing points and six (6) newly established points. The acquired GNSS data was processed using the South GNSS Processor software to obtain ellipsoidal heights. Precise leveling data was processed using the Leica Geo-Office Software, and a Microsoft Excel program was developed to adjust the data using the ob-

servation equation method for leveling network adjustment, resulting in orthometric heights. The UAV data was processed using DJI Pix4D Enterprise software to generate point cloud data, 3D mesh, digital terrain models (DTMs), and orthomosaic. The point cloud, consisting of at least eighteen thousand (18,000) points with ellipsoidal and orthomet-

ric heights, was used to calculate the geoidal height for each point. The coordinates (eastings and northings) and geoidal heights were imported into Surfer software to create a contour-based model. This model allows for obtaining the geoidal height of any point within the study area by inputting the corresponding easting and northing coordinates.

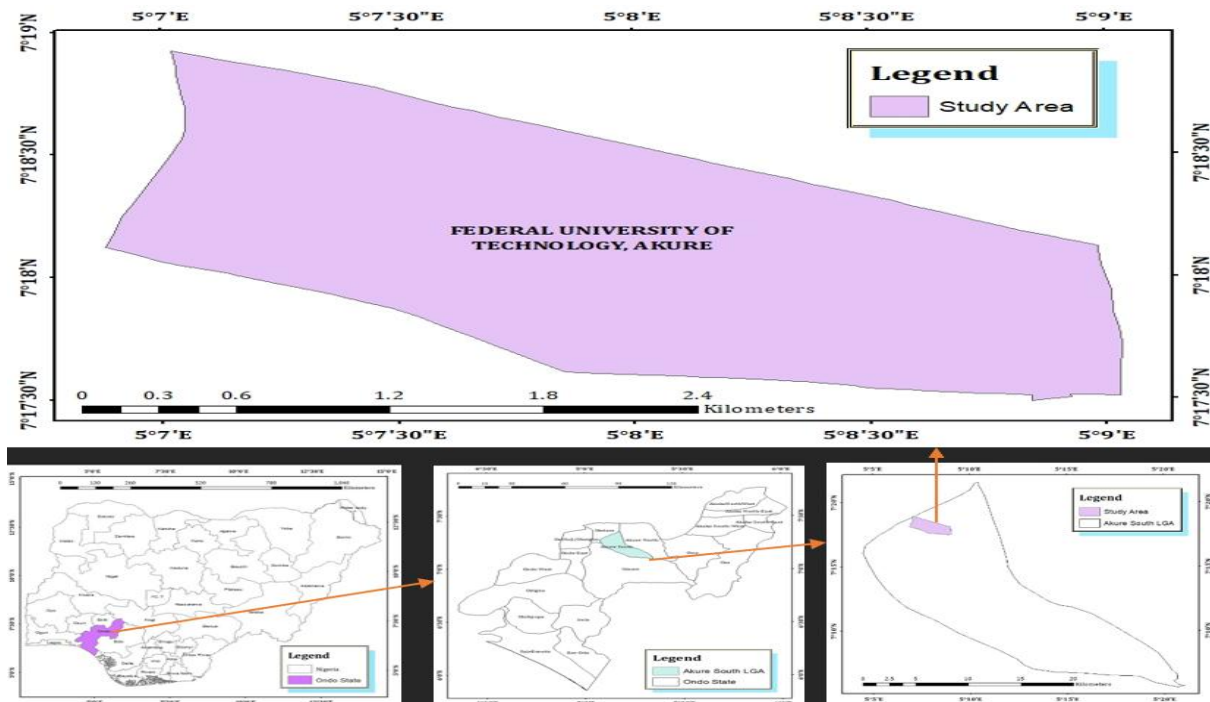


Fig. 2. Study area

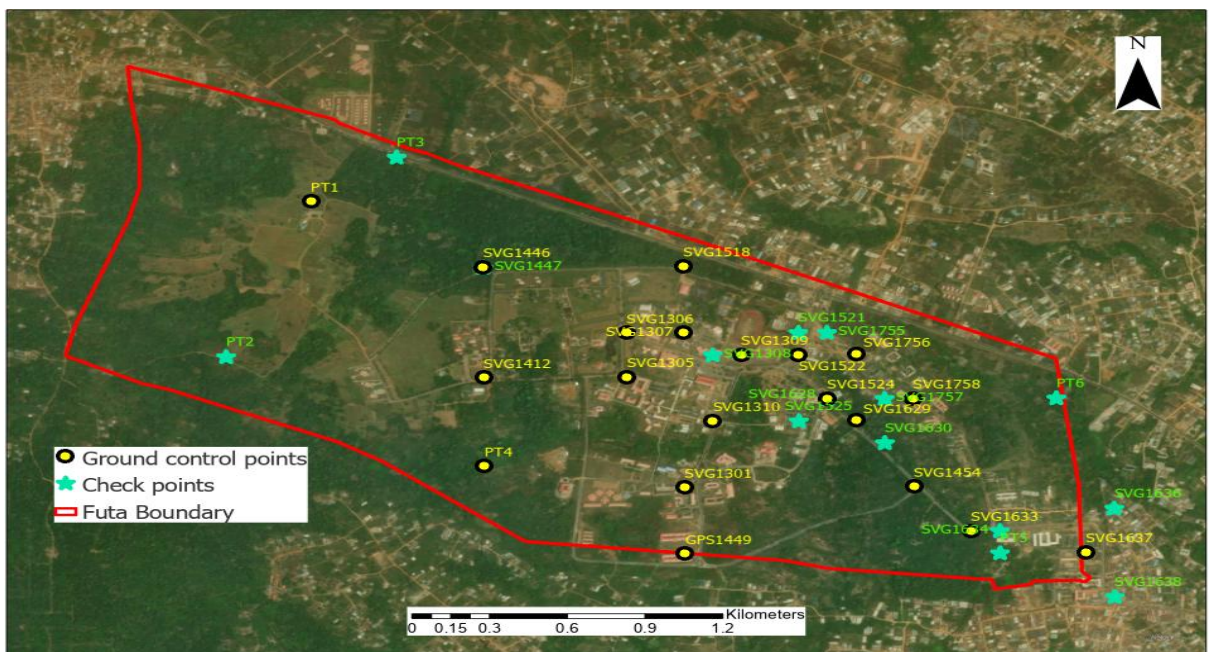


Fig. 3. Distribution of ground control points in the study area

GNSS observation

A total of thirty-five (35) GCPs in the study area were observed using South differential Global Positioning System (DGPS). The existing ones (29 in total) were observed to confirm their position's stability, while six (6) new points were established and observed to ascertain their geographic coordinates and ellipsoidal heights. The observations were carried out in static mode, with a minimum duration of thirty (30) minutes for each existing station and maximum of one (1) hours for each of the new station with five (5) seconds epoch rate to monitor a sufficient number of satellites, thereby improving the data streaming quality and ensuring greater accuracy. The obtained accuracy of the GNSS observations is 10 mm, demonstrating the vertical precision achieved through satellite-based positioning.

Precise levelling observation

The orthometric heights of the six (6) newly established GCPs were determined using a precise geometric levelling technique with the Leica DNA03 digital level instrument. To ensure the instrument's quality and accuracy, a two-peg test was performed, revealing a collimation error of 0.002 mm and confirming the instrument's excellent condition for observations. To achieve higher accuracy, a total of six (6) loops were conducted, covering twelve (12) lines and seven (7) points.

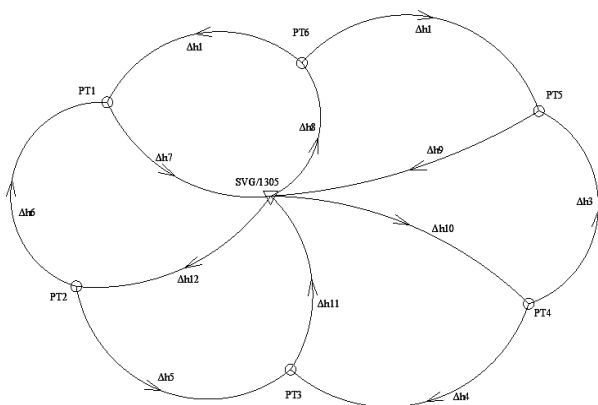


Fig. 4. The levelling loop

The SVG/1305 benchmark was utilized as the reference point, as shown in Fig. 4 Each section of the levelling survey had a maximum distance of sixty (60) meters, with thirty (30) meters measured from the instrument position to both the back and foresight points. The reduced levels of the new points and their change in height from the were

adjusted using observation equation method of levelling network adjustment and corrections was done to obtain the final orthometric heights. The accuracy obtained for the levelling measurements in this study is 1.3 mm, indicating the vertical precision achieved through this traditional surveying technique.

UAV mapping

To collect data on surface properties such as vegetation, elevation, and ground subsidence, we used a DJI Phantom 4 Pro UAV and the orthomosaic and digital surface model of the study area were generated. The UAV flight was conducted at a height of 150m above ground level, with a forward overlap of 60% and a camera angle of 90°. For accurate georeferencing, a total of 20 GCPs were used. The positions of these GCPs were collected using a South differential Global Positioning System (DGPS), while their orthometric heights were determined through precise levelling techniques.

UAV data processing

The 3,737 images captured by the drone were imported into the DJI Pix4DEnterprise environment. These images underwent photo alignment processing to enhance the optimization of key points, tie points, and the estimation of photo match points. Subsequently, 35 Ground Control Points (GCPs), which were acquired using the South DGPS instrument, served as reference points to improve the camera positions and orientation. Of these GCPs, 20 were utilized for bundle adjustment, while the remaining 15 GCPs were designated as checkpoints. The process of creating a dense point cloud and a 3D mesh commenced with the generation of essential points required for constructing the terrain model. The point cloud data were interpolated to generate a digital terrain model. The final step involved the creation of the orthomosaic depicted in Fig. 5, which was achieved through the orthorectification of the generated digital terrain model.

Generation of DTMs from point cloud data

The Digital Terrain Model (DTM) generation process commenced with the careful georeferencing of UAV-derived images. The georeferencing process involved the incorporation of both ellipsoidal and orthometric heights to ensure accurate horizontal and vertical positioning with the vertical datum set to World Geodetic System 1984 (WGS84). Following georeferencing, a pre-processing step was im-

plemented to filter the UAV-derived point cloud data. This filtering process involved selectively removing non-ground points such as vegetation

canopy and structures so as to ensure that the resulting DTM accurately reflected the topographical surface.



Fig. 5. Orthomosaic imagery of the study area

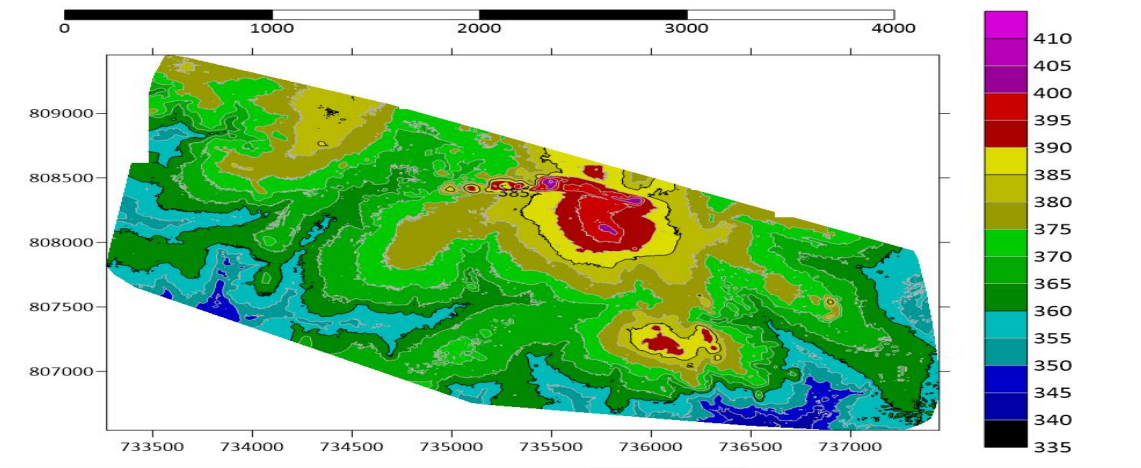


Fig. 6. DTM-generated contour map from ellipsoidal heights

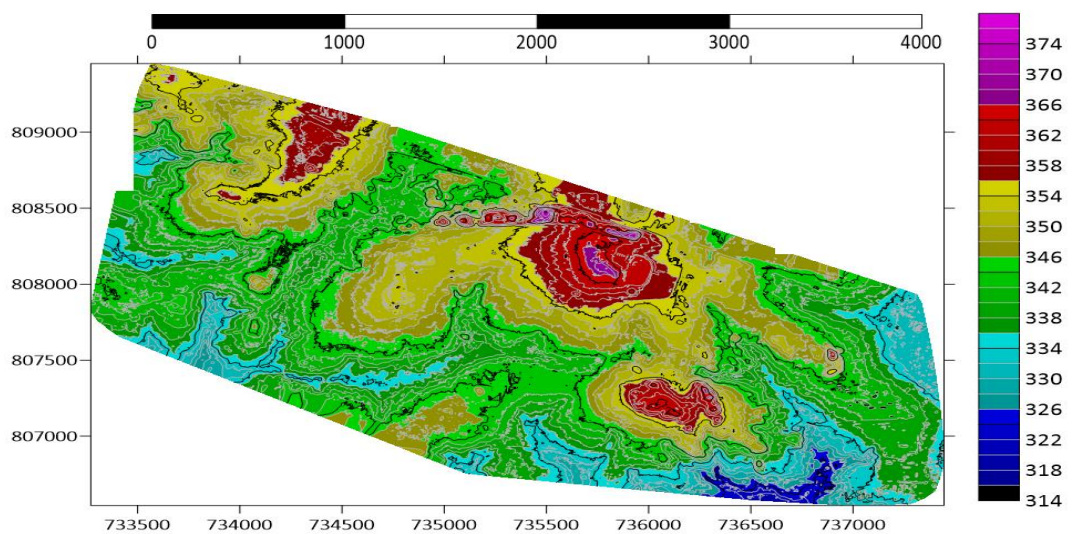


Fig. 7. DTM-generated contour map from orthometric heights

In the point cloud data filtering process, the average spatial distance of each point to its neighboring points is estimated. The distribution of differences between calculated distances and their average is assumed to follow a Gaussian distribution (Erol et al., 2020). Points with distance differences that deviate from this distribution are identified as outliers and removed. This removal is based on a specified maximum distance criterion, ensuring that points farther than the defined maximum distance are considered blunders and subsequently excluded.

Following the removal of blunders, the data undergo denoising through an elevation thresholding method. Specifically, the threshold was set as the sum of the mean height and the standard deviation of the height. Thus, after filtering the data difference from their mean. Five neighboring points were chosen for the application of these filtering processes. Subsequently, 27 % of all points were removed from the point cloud derived from the UAV mapping. After filtering the data, a regular grid covering the study area was generated and kriging interpolation was employed to estimate elevations at grid points for creating ellipsoidal and orthometric DTMs using Surfer 20 software. Fig 6. and 7 shows the DTM-generated contour map from ellipsoidal and orthometric heights.

Computation of the UAV-derived geoid model

The geoidal undulation for all the points in the study area was determined using the ellipsoidal and orthometric heights model generated from the point cloud of over 18,000 points. A program was written in a Microsoft Excel spreadsheet according to the equation below to compute the geoidal undulations with respect to WGS84.

$$N^{UAV} = h^{UAV} - H^{UAV} \quad (1)$$

In order to test the validity of the method used in this study, fifteen (15) GCPs were set aside as check points out of the thirty-five (35) GCPs. So, the ellipsoidal, orthometric, and geoidal heights of the twenty (20) GCPs over the study area were computed using the Microsoft excel worksheet.

Root Mean Square Error

In order to check the accuracy and reliability of the geoidal undulations computed in this study, the root mean square error (RMSE) is employed. The RMSE estimates the difference between the observed values and the predicted values. Thus, the

RMSE between the geoidal undulations obtained from existing data and the predicted geoidal undulations from UAV-generated data is estimated as:

$$RMSE = \sqrt{\frac{\sum_{i=1}^n (O_i - P_i)^2}{N}}, \quad (2)$$

where O_i is the geoidal undulations obtained through existing data, P_i is the predicted geoidal undulations from UAV, and N is the number of points.

Results

In diverse geographical contexts, researchers have adopted a range of techniques to model the geoid. Each technique comes with its own unique merits and limitations. In the present study, we explore an innovative approach to geoid modelling by harnessing the capabilities of UAVs. This approach offers the distinct advantage of efficiently covering extensive areas within a shorter timeframe. The results of the UAV-derived ellipsoidal, orthometric, and geoidal undulations for twenty (20) ground control points that were used in creating the model are presented in Table 1. The geoidal undulation results of the final fifteen (15) GCPs, which were determined by incorporating the coordinate and ellipsoidal height obtained from the GPS observation into the model, are shown in Table 2 as a means of validating the geoid model and an RMSE of 0.113 is obtained.

Visual representations of our findings are presented in Fig. 8 and 9. Fig. 8 portrays a UAV-generated contour map, providing a visual understanding of the terrain's characteristics. Meanwhile, Fig. 9 offers a three-dimensional representation of the geoid model for the study area. The model shows that the geoidal height values in the study area are all positive ranging between 17.5 m to 32.5 m at 5 m grid interval with the highest values more prominent in the Northern part of the area while the lowest values are prominent in the Southwestern part of the area. The geoid undulation within the study area experiences variations influenced by both the gentle slope of the topography and the heterogeneous mass distribution of the earth's surface. These variations are primarily due to the ongoing developmental changes that have occurred within the school since its establishment in 1981. As the institution has seen increased structural development over the years, these changes in mass distribution have led to corresponding shifts

in gravity values at various locations, further influencing the geoid undulation observed in our model. It is important to note that an area with a complex topography (comprising of lowland and hilly terrains), such as the one under investigation, are

known for exhibiting substantial geoid variations due to the irregular distribution of mass, geological features, and topographical changes. Thus, the observed geoid variation aligns with expectations for such terrain types.

Table 1

UAV-derived heights for the ground control points

Station	Geographic Coordinates		UAV Acquired Heights (m)		UAV-Derived Geoidal Undulations (m)
	Latitude	Longitude	Ellipsoidal Height (m)	Orthometric Height (m)	
SVG1301	7.29842	5.13533	375.746	348.637	27.109
SVG1305	7.30342	5.13283	378.862	350.787	28.075
SVG1306	7.30536	5.13273	385.458	356.015	29.443
SVG1307	7.30451	5.13486	392.514	361.592	30.922
SVG1309	7.30354	5.13698	384.519	354.699	29.820
SVG1310	7.30105	5.13601	374.892	347.723	27.169
SVG1412	7.30325	5.12816	374.160	347.625	26.535
SVG1446	7.30810	5.12793	372.356	345.861	26.495
GPS1449	7.29488	5.13544	361.789	336.843	24.946
SVG1454	7.29840	5.14305	360.754	336.483	24.271
SVG1518	7.30831	5.13455	393.490	362.427	31.063
SVG1522	7.30381	5.13895	382.575	353.650	28.925
SVG1524	7.30231	5.13975	377.069	348.960	28.109
SVG1629	7.30103	5.14089	371.818	344.010	27.808
SVG1633	7.29649	5.14465	357.020	333.646	23.373
SVG1637	7.29473	5.14948	361.265	337.817	23.448
SVG1756	7.30354	5.14069	375.458	347.855	27.603
SVG1758	7.30246	5.14311	375.287	347.893	27.394
PT1	7.31078	5.12196	379.106	354.981	24.126
PT4	7.29915	5.12835	361.199	338.008	23.191

Table 2

Geoidal Undulations derived from the model for the check points

Station	Geographic Coordinates		Existing Geoidal Undulations (m)	UAV-Derived Geoidal Undulations (m)	Difference (m)
	Latitude	Longitude			
SVG1308	7.30387	5.13579	30.137	30.219	-0.082
SVG1447	7.30812	5.12844	26.825	26.945	-0.120
SVG1521	7.30514	5.13924	29.171	29.365	-0.194
SVG1525	7.30124	5.13944	27.871	27.761	0.111
SVG1628	7.30219	5.14010	27.640	27.420	0.220
SVG1630	7.29983	5.14203	25.416	25.523	-0.107
SVG1634	7.29638	5.14603	23.545	23.461	0.085
SVG1636	7.29660	5.14952	23.626	23.656	-0.030
SVG1638	7.29306	5.14968	22.827	22.796	0.031
SVG1755	7.30466	5.14011	28.527	28.495	0.031
SVG1757	7.30202	5.14222	26.734	26.838	-0.104
PT2	7.30387	5.11935	20.873	20.694	0.179
PT3	7.31250	5.12503	25.005	25.014	-0.009
PT5	7.29453	5.14587	22.070	22.152	-0.082
PT6	7.30238	5.14817	25.132	25.084	0.048
				RMSE =	0.113

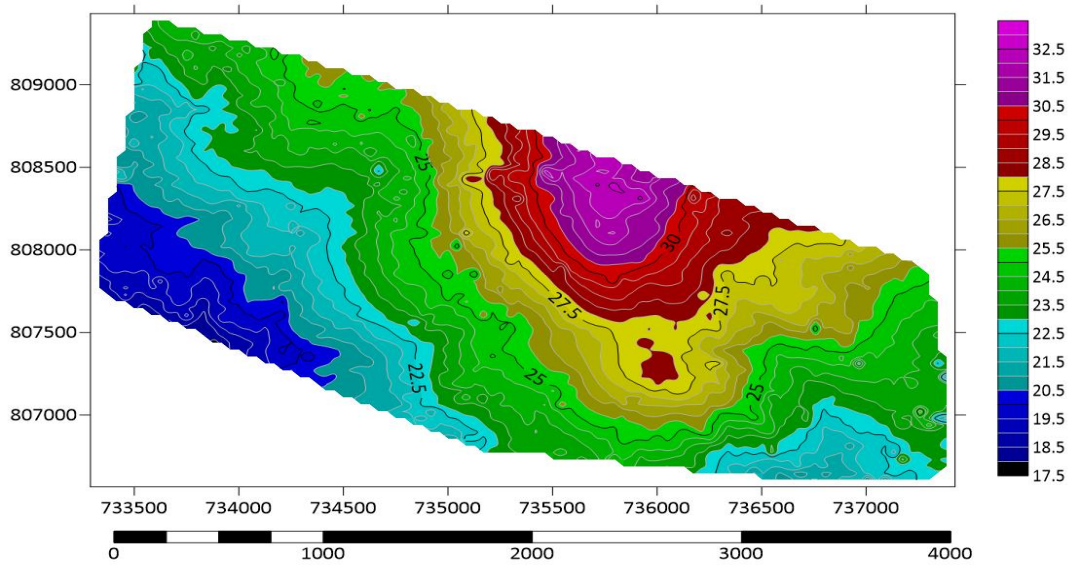


Fig. 8. UAV-generated geoidal map of the study area

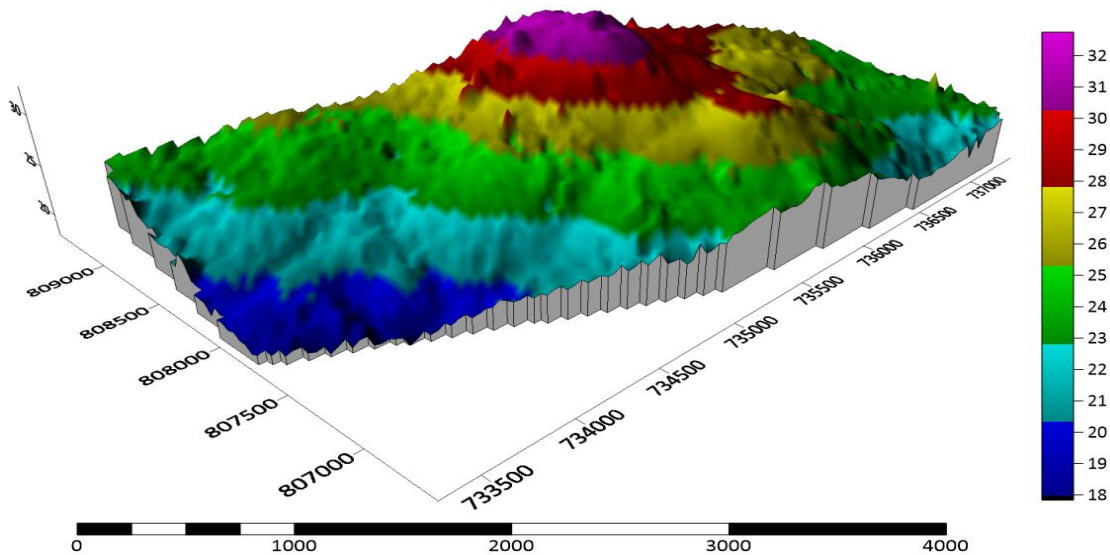


Fig. 9. 3D UAV-generated geoidal model of the study area

Hypothesis testing

In this study, hypothesis testing was conducted on the check point data using t-distribution statistics in a Microsoft Excel spreadsheet. The objective of the hypothesis was to examine whether there is a significant difference between the mean geoidal undulations obtained from UAV mapping and those obtained from the geodetic method, with a significance level of 5%. The hypotheses tested were as follows:

H_0 = The mean geoidal undulation estimated from UAV mapping is equal to the mean geoidal undulation estimated from the geodetic method.

H_1 = The mean geoidal undulation estimated from UAV mapping is not equal to the mean geoidal undulation estimated from the geodetic method.

The decision rule stated that if $t_{cal} > t_{tab}$ at a 0.05 significance level, we reject H_0 and accept H_1 . However, since $t_{cal} < t_{tab}$ for both the one-tail and two-tail tests (specifically, $0.480 < 1.761$ in the one-tail test and $0.961 < 2.145$), we accept H_0 . This indicates that although there are slight variations in the geoidal heights obtained from the existing and UAV-generated data in the study area, these variations are not statistically significant. Thus, the accuracy of the UAV-derived geoid model is confirmed.

***Comparison of geoidal undulation differences:
UAV vs existing geometric and global geoids***

In this study, we compared the geometric geoid model estimated from UAV data with both an existing polynomial geoid model and the Earth Gravitational Model 2008 (EGM08). The statistics derived from these analyses provide insights into the fitting performance of the compared models. The polynomial geoid model, developed by Raufu and Tata (2021) using high-accuracy GNSS/levelling data co-

vering the Akure region, reported a standard deviation of 14.7 cm for the best-fitting geoid model. Herbert and Olatunji (2021) also assessed the accuracy of estimating orthometric height in the study area using GNSS and EGM data, reporting standard errors of 1.361 m, 1.365 m, and 1.367 m for the EGM08, EGM96, and EGM84, respectively. Therefore, in terms of accuracy the UAV-geoid model estimated in this study is considered comparable to the existing polynomial and EGM08 geoid models.

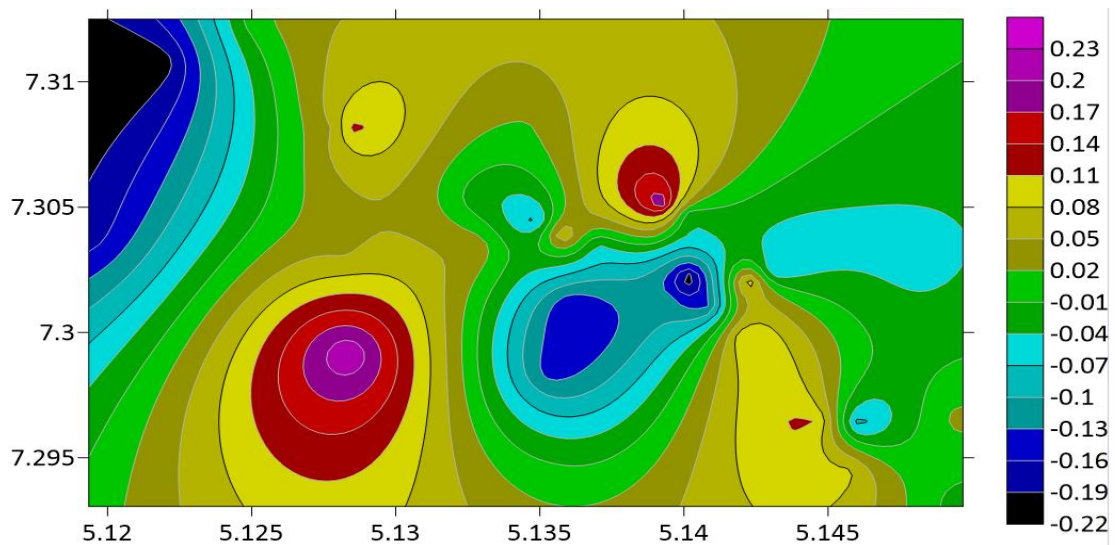


Fig. 10. Map of the difference between UAV-generated and existing geometric geoidal model of the study area

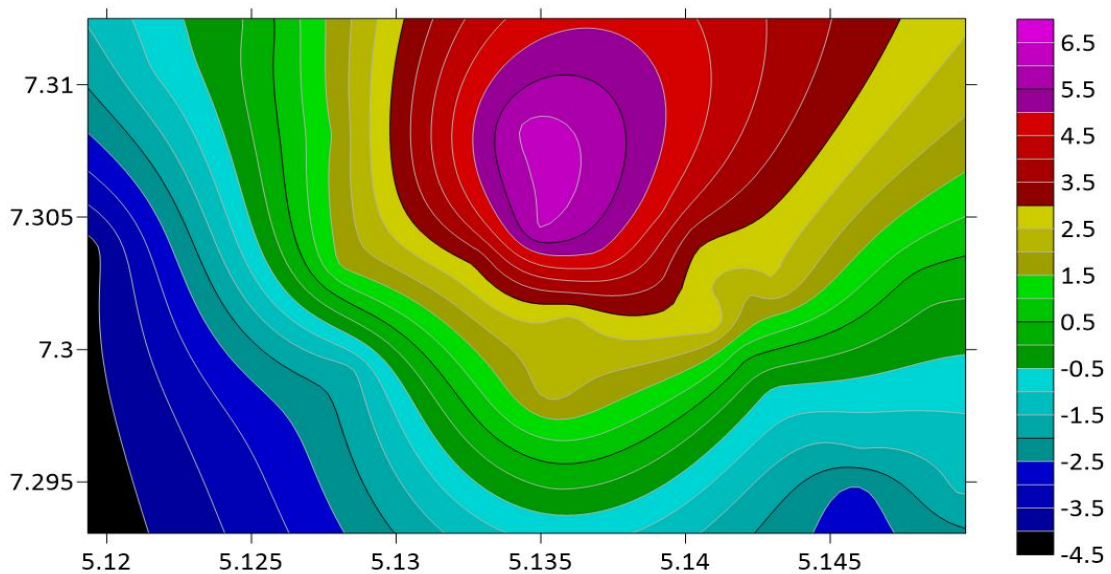


Fig. 11. Map of the differences between UAV-generated and EGM08 geoidal model of the study area

Table 3 shows the statistical differences in geoidal undulations estimated from the UAV compared to existing geometric and global geoid models at selected geodetic control points while Fig. 10 and 11 shows the visual differences respectively. The results indicate that the differences in geoidal undulation between the UAV-geoid and the existing polynomial geoid model range from -22 cm to 23 cm, with a mean value of -1.2 cm and an RMSE value of 10.9 cm. Furthermore, the differences in geoidal undulation between the UAV-geoid and EGM08 range from -42.1 dm to 61.5 dm, with a mean value of 15.5 dm and an RMSE value of 25.9 dm respectively. The statistical evaluation suggests that the fit of the global geoid to the local geoid model is not superior when compared to the existing polynomial geoid model in the study area.

Table 3

Statistical differences between UAV-geoid and existing geometric and global geoids (EGM08)

Geoidal undulation differences	Minimum (m)	Maximum (m)	Mean (m)	RMS E (m)
UAV-geoid vs existing polynomial geoid	-0.220	0.230	-0.012	0.109
UAV-geoid vs EGM08	-4.207	6.152	1.545	2.590

The scientific novelty and practical significance

The research showcases the scientific importance of employing UAV technology for geoid modelling, offering a cost-effective, high-precision solution that can have practical applications in various domains. This novel approach not only advances geodetic surveying techniques but also holds promise for applications in various domains. By leveraging UAV technology, this research opens new possibilities for professionals and researchers in geospatial sciences and related fields, providing valuable insights for real-world problem-solving and decision-making.

Conclusions

The paper investigates the use of unmanned aerial vehicle (UAV) technology for local geoid modelling. Imagery of the study area was captured by the UAV at a flying height of 150 m. A total of thirty-five (35) points with ellipsoidal and orthometric height values were utilized to georeference the UAV images, with twenty (20) points serving as ground control points (GCPs) and fifteen (15) as validation points. Point clouds data derived from the UAV were used to generate DTM for ellipsoidal and orthometric heights. The geoidal undulation was calculated as the difference between the UAV-derived ellipsoidal and orthometric heights, leading to the development of a local geoid model for the study area. The analysis resulted in a root mean square error value of 0.113 m when comparing the existing and UAV-derived geoidal heights. Hypothesis testing supported the null hypothesis, indicating no significant difference between the two models at a 5% significance level. Further comparison between the UAV-derived geoid with the existing polynomial geoid and EGM08 model indicated that the polynomial geoid fitted better compared to the EGM08 with RMSE of 10.9 cm. Notably, DTMs obtained through remote data collection with UAV have a great benefit in geoid determination because they capture all geoid features in high detail. This study highlights the suitability of UAV technology for achieving centimeter-level accuracy in determining geoidal undulations within smaller areas for localized purposes. While this approach facilitates the creation of a local geoid model with enhanced accuracy in regions characterized by complex topography, it is acknowledged that the obtained accuracy is not enough for large-scale engineering and mapping applications. To address this limitation, it is recommended to conduct additional data analysis and employ diverse numerical methods for more comprehensive geoid modelling, particularly in larger areas. Furthermore, future research initiatives should explore the potential enhancement of height accuracies by integrating innovative

data sources and technologies. Exploring the synergistic potential of various remote sensing techniques, including the integration of photogrammetric imagery, Lidar data, and advanced methods like Interferometric Synthetic Aperture Radar (InSAR), along with employing Unmanned Aerial Vehicle (UAV) technology, could present novel avenues for precise height determination. Furthermore, the development of tailored strategies to harness the strengths of these combined approaches is crucial for achieving superior results. This comprehensive approach is expected to significantly advance our understanding and modelling of local geoids, especially when leveraging the capabilities of photogrammetric techniques.

REFERENCES

- Agajelu, S.I. (2018). *Geodesy: The Basic Theories – Classical & Contemporary*. Enugu, El 'Demak Publishers, ISBN 978-978-8436-99-0, pp. 4, 5, 9, 11 – 21
- Albayrak, M., Özlüdemir, M.T., Aref, M.M., & Halicioglu, K. (2020). Determination of Istanbul geoid using GNSS/levelling and valley cross levelling data. *Geodesy and Geodynamics*, 11(3), 163-173.
- Al-Krargy, E. M., Doma, M. I., & Dawod, G. M. (2014). Towards an Accurate Definition of the Local Geoid Model in Egypt using GPS / Levelling Data: A Case Study at Rosetta Zone. *International Journal of Innovative Science and Modern Engineering (IJISME)*, 2(11).
- Belay, E. Y., Godah, W., Szelachowska, M., & Tenzer, R. (2021). ETH-GM21: A new gravimetric geoid model of Ethiopia developed using the least-squares collocation method. *Journal of African Earth Sciences*, 183,104313.
- Chi, Y.Y., Lee, Y.F., & Tsai, S.E. (2016). Study on High Accuracy Topographic Mapping via UAV-based Images. *IOP Conference Series: Earth and Environmental Science*, 44, 032006.
- Christiansen, M. P., Laursen, M. S., Jørgensen, R. N., Skovsen, S., & Gislum, R. (2017). Designing and testing a UAV mapping system for agricultural field surveying. *Sensors*, 17(12), 2703.
- Erol, S., Özögel, E., Kuçak, R. A., & Erol, B. (2020). Utilizing Airborne LiDAR and UAV Photogrammetry Techniques in Local Geoid Model Determination and Validation. *ISPRS International Journal of Geo-Information*, 9(9), 528. doi:10.3390/ijgi9090528
- Erol, S., & Erol, B. (2020). A comparative assessment of different interpolation algorithms for prediction of GNSS/levelling geoid surface using scattered control data. *Measurement*, 173, 108623.
- Gonzalez, L. F., Montes, G. A., Puig, E., Johnson, S., Mengersen, K., & Gaston, K. J. (2016). Unmanned aerial vehicles (UAVs) and artificial intelligence revolutionizing wildlife monitoring and conservation. *Sensors*, 16(1), 97.
- Herbert, T. & Olatunji, R.I. (2021). Determination of orthometric height using GNSS and EGM Data: A scenario of the Federal University of Technology Akure. *International Journal of Environment and Geoinformatics (IJECEO)*, 8(1):100-105. doi: 10.30897/ijegeo.754808
- Jekeli, C., Yang, H. J., & Kwon, J. H. (2012). The offset of the South Korean vertical datum from a global geoid. *KSCE Journal of Civil Engineering*, 16(5), 816–821. doi:10.1007/s12205-012-1320-3
- Maglione, P., Parente, C., & Vallario, A. (2018). Accuracy of global geoid height models in local area: Tests on Campania region (Italy). *International Journal of Civil Engineering and Technology*, 9, 1049-1057.
- National Oceanic and Atmospheric Administration, NOAA. (2021). Is the Earth round? retrieved from National Ocean Service website, 2021, <https://oceanservice.noaa.gov/facts/eutrophication.html>,
- Odera, P. A., & Fukuda, Y. (2015). Recovery of orthometric heights from ellipsoidal heights using offsets method over Japan. *Earth, Planets and Space*, 67(1).
- Oluyori, P. D., Ono, M. N., & Eteje, S. O. (2018). Comparison of Two Polynomial Geoid Models of GNSS/Leveling Geoid Development for Orthometric Heights in FCT, Abuja. *International Journal of Engineering Research and Advanced Technology (IJERAT)*, 4(10), 1-9.
- Polat, N., & Uysal, M. (2017). DTM generation with UAV based photogrammetric point cloud. *ISPRS - International Archives of the Photogrammetry, Remote Sensing and Spatial Information Sciences*. XLII-4/W6, 77-79.
- Prasad, S. (2015). Basic Geodesy Unit: II Semester: I Paper Code: GIS 05: Name of Paper: Earth Positioning System, PG Diploma in RS & GIS.
- Quaye-Ballard, N.L., Asenso-Gyambibi, D., & Quaye-Ballard, J. (2020). Unmanned Aerial Vehicle for Topographical Mapping of Inaccessible Land Areas in Ghana: A Cost-Effective Approach. Presented at the 2020 FIG Working Week, Amsterdam, Netherlands, May 10– 14.

- Raufu, I. O., & Tata, H. (2021). Accuracy Assessment of Different Polynomial Geoid Models in Orthometric Height Determination for Akure, Nigeria. *Geodetski glasnik*, 52, 61-73.
- Sansò, F., Reguzzoni, M., & Barzaghi, R. (2019). *Geodetic Heights*. Springer Nature, Switzerland, <https://doi.org/10.1007/978-3-030-10454-2>.
- Turner, I. L., Harley, M. D., & Drummond, C. D. (2016). UAVs for coastal surveying. *Coastal Engineering*, 114, 19–24
- Yeh, F.H., Huang, C.J., Han, J.Y., & Ge, L. (2018). Modeling Slope Topography Using Unmanned Aerial Vehicle Image Technique. *MATEC Web of Conferences*, 147, 07002. doi:10.1051/mateconf/201814707002.

Ібрагім Олатунджі RAUFU^{1A*}, Герберт ТАТА^{1B}, Соліху ОLAOSEGBA²

¹ Департамент геодезії та геоінформатики, Федеральний технологічний університет, Акуре, Нігерія, raufuibrahimolatunji@gmail.com, htata@futa.edu.ng, ^{1A}<https://orcid.org/0000-0003-3474-8618>, ^{1B}<https://orcid.org/0000-0002-9755-1612>

² Кафедра геодезії та геоінформатики, Федеральна школа геодезії Ойо, Нігерія, olaosegba@fss-oyo.edu.ng,

²<https://orcid.org/0000-0002-6212-1081>

МОДЕЛЮВАННЯ ЛОКАЛЬНИХ ГЕОЇДНИХ УНДУЛЯЦІЙ
ЗА ДОПОМОГОЮ БЕЗПЛОТНИХ ЛІТАЛЬНИХ АПАРАТІВ (БПЛА):
ПРИКЛАД ФЕДЕРАЛЬНОГО ТЕХНОЛОГІЧНОГО УНІВЕРСИТЕТУ, АКУРЕ, НІГЕРІЯ

Дослідження було спрямоване на розробку моделі геоїда з використанням технології безпілотних літальних апаратів (БПЛА). Для цього використано БПЛА для отримання зображень досліджуваної території з висоти 150 м із роздільною здатністю на Землі 4,19 см. Всього отримано 3737 зображень, які охоплюють площу 725,804 га. Існуючі еліпсоїдні та ортометричні висоти були використані для географічної прив'язки отриманих зображень. Для аналізу використано 35 точок, з яких 20 точок визначено як наземні контрольні точки (GCP), а решта 15 точок – контрольні точки (CPs). Використовуючи отримані з БПЛА цифрові моделі рельєфу (DTMs), створено набір даних, що містить 18 492 точки як для еліпсоїдальної (h), так і для ортометричної (H) висот. Різниця між цими висотами, які називаються висотами геоїда (N), були розраховані як $N = h - H$ для всіх 18 492 точок. Ці висоти геоїда згодом використані для створення моделі геоїда, включаючи контурні карти та 3D-карти досліджуваної території. Щоб оцінити точність висот геоїда, отриманих за допомогою БПЛА, виконано аналіз середньоквадратичної помилки (RMSE) шляхом порівняння їх з існуючими висотами геоїда, і встановлено, що вона становить 0,113 м. Наукова новизна та практична значущість полягає в розробці локальної моделі геоїда досліджуваної території з точністю до сантиметра. Таким чином, результати цього дослідження можуть бути використані для широкого спектру застосувань, включаючи землеустрій, будівництво та оцінку впливу на навколишнє середовище на території дослідження.

Ключові слова: геоїд, БПЛА, цифрові моделі рельєфу, еліпсоїдальна висота, ортометрична висота

Received 20.10.2023